Bonache Bezares, V.; Salvador Moya, MD.; Fernández Valdés, A.; Borrell Tomás, MA. (2011). Fabrication of full density near-nanostructured cemented carbides by combination of VC/Cr3C2 addition and consolidation by SPS and HIP technologies. International Journal of Refractory Metals and Hard Materials. 29(2):202-208. doi:10.1016/j.ijrmhm.2010.10.007.

Fabrication of full density near-nanostructured cemented carbides by combination of VC/Cr_2C_3 addition and consolidation by SPS and HIP technologies

V. Bonache[1*], M.D. Salvador[1], A. Fernández[2], A. Borrell[3]

[1]Instituto de Tecnología de Materiales (ITM). Universidad Politécnica de Valencia. Camino de Vera, s/n, 46022 Valencia, Spain

[2]Fundación ITMA, Parque Tecnológico de Asturias, 33428 Llanera (Asturias), Spain

[3]Centro de Investigación en Nanomateriales y Nanotecnología (CINN) (Consejo Superior de Investigaciones Científicas - Universidad de Oviedo - Principado de Asturias), Parque Tecnológico de Asturias, 33428 Llanera (Asturias), Spain

*Corresponding Author:

Name: Bonache Bezares, Victoria

Phone: +34 692512435

Fax: +34 963877629

E-mail: vicbobe@doctor.upv.es

Postal Address:

Instituto de Tecnología de Materiales

Edif. 5E. 1ª Planta

Universidad Politécnica de Valencia

Camino de Vera s/n. E-46022

Valencia, Spain.

Abstract

The aim of present work is to study the effect of VC and/or Cr_2C_3 in densification, microstructural development and mechanical behavior of nanocrystalline WC-12wt.%Co powders when they are sintered by spark plasma sintering (SPS) and hot isostatic pressing (HIP). The results were compared to those corresponding to conventional sintering in vacuum. The density, microstructure, X-ray diffraction, hardness and fracture toughness of the sintered materials were evaluated. Materials prepared by SPS exhibits full densification at lower temperature (1100 ºC) and a shorter stay time (5 min), allowing the grain growth control. However, the effect of the inhibitors during SPS process is considerably lower than in conventional sintering. Materials prepared by HIP at 1100 ºC and 30 min present full densification and a better control of microstructure in the presence of VC. The added amount of VC allows obtaining homogeneous microstructures with an average grain size of 120 nm. The hardness and fracture toughness values obtained were about 2100 HV_{30} and close to 10 MPa $m^{1/2}$, respectively.

Keywords: WC–Co cemented carbides; nanocrystalline powders; grain growth inhibitors; SPS; HIP.

Introduction

WC-Co hardmetals are widely used as cutting tools and dies due to their high wear resistance and toughness [1-3]. Manufacturing WC-Co cemented carbides with fine grain size even nanometer scale is a good method to improve its properties. As an example, hardness and strength of WC-Co hardmetals can be improved by decreasing the WC grain size to the nanometer scale. However, the production of bulk

nanocrystalline (grain sizes <100 nm) cemented tungsten carbide remains a technological challenge because of their fast grain growth during sintering.

The consolidation of nanostructured WC-Co powder has been studied using a variety of techniques including the standard liquid phase sintering (LPS) [4-9], hot isostatic pressing (HIP) [10], unconventional processes such as microwave sintering [11,12] and spark plasma sintering (SPS) [13-18], high frequency induction-heated sintering (HFIHS) [19-21], rapid omni compaction (ROC) [22], pulse plasma sintering (PPS) [23] and ultrahigh pressure rapid hot consolidation (UPRC) [24]. Due to the high temperature during sintering, grain growth occurs very quickly and it explains that the finest average grain sizes of sintered WC-Co reported in the literature up to date, using nanograined powders, is around 200-300 nm. Considerable efforts have been dedicated to study the densification and grain growth control during sintering of the nanosized WC-Co powders in order to achieve the goal of obtaining fully dense nanostructured WC-Co materials.

One of the keys for controlling the grain growth of WC-Co composites is a suitable selection of additives as grain growth inhibitors. Vanadium carbide (VC) and chromium carbide (Cr_3C_2) are the most effective grain growth inhibitors for this system thanks to their high solubility and mobility in cobalt phase at low temperatures [25-27].

Moreover, the grain growth can be inhibited by using special sintering technologies allowing very high heating rates, increasing the densification rate, even at lower sintering temperature and shorter holding times, such as microwave sintering [28], rapid hot pressing sintering [12,29], spark plasma sintering (SPS) [30], and so on. In this sense, spark plasma sintering, that is also known as pulse electric current sintering

(PECS), is a newly developed sintering method, which enables a powder compact to be sintered by passing high pulsed electric current through the compact. It has been successfully used for composites, functionally graded materials and nanocrystalline materials. It is therefore highly interesting to investigate the effect of grain growth inhibitors on the WC grain growth and its mechanical properties when they are combined with the use of PECS sintering technique [31].

In this paper, nanocrystalline WC-Co powders with different additions of VC/Cr_3C_2 inhibitors were fully densified by SPS and HIP sintering methods at 1100 ºC. The effect of the amount of inhibitor in the density, microstructure, hardness and fracture toughness were investigated and compared with conventional sintering in vacuum at 1400 ºC.

Experimental procedure

The mixture used in this work was nanocrystalline WC-12Co powders with WC particle size of 30-80 nm, manufactured by Inframat Advanced Materials. The appropriate amounts of vanadium carbide (VC) and chromium carbide (Cr_2C_3) were added to the raw powders, which were used as grain growth inhibitors. Free Carbon was added to all compositions in order to adjust final C content in the sintered samples. Designation and compositions of the final powder mixtures are shown in Table 1.

The mixtures were milled for 2 h in a Fritsch Pulverisette 7 planetary ball mill using isopropyl alcohol as the liquid medium and under protective Argon atmosphere. The ball-to-powder weight ratio was 10:1 and the rotation speed was 700 rpm. 2.5 wt.% of polyethylene glycol (PEG 1500) was used as organic binder in the mixtures

consolidated by HIP and vacuum. After wet milling, powder mixes were dried at 110 ºC during 2 h under Argon atmosphere.

SPS sintering: The powder samples were placed into a graphite die with an inner diameter of 20 mm and cold uniaxially pressed at 30 MPa. Then, they were introduced in a spark plasma sintering apparatus HP D 25/1 (FCT System) under low vacuum (10-1 mbar) and sintered at 1100 ºC for 5 min under an applied pressure of 80 MPa and a heating rate of 100 ºC min^{-1}.

HIP and vacuum sintering: Green compacts were prepared by uniaxial pressing at 200 MPa into a matrix with an inner diameter of 5 mm and were consolidated by two routes: vacuum sintering at 1400 ºC for 30 minutes (heating rate of 10 ºC min^{-1}), in a high vacuum Carbolite furnace (VS: 10^{-4} mbar), and glass-encapsulated HIPing (GEHIP) at 1100 ºC for 30 minutes and 120 MPa pressure (heating rate of 30 ºC min^{-1}) using a HIP 2000 EPSI N.V system. In the two sintering routes, a previous step where the organic binder is burned out in a vacuum furnace at 450 ºC for 60 minutes (heating rate of 3 ºC min^{-1}) was included.

Powders morphology and microstructures of the sintered materials have been characterized by field emission scanning electron microscopy (FESEM). The consolidated materials densities were measured following the Archimedes' method with ethanol immersion, according to ISO 3369 standard. The porosity has been analyzed by quantitative metallographic of polished surfaces according to ISO 4505 standard, where A00, A02, A04, A06 codes correspond to 0.02, 0.06, 0.2, 0.6 vol.% porosity, respectively (for pore sizes below 10 microns). Similar codes are assigned to B type porosity (pores in the range of 10-25 microns). The WC grain size was measured using

two methods: lineal intercept method, following standard ASTM E112 and image analysis Image-Pro Plus software that also allowed obtaining grain size distributions.

Vickers hardness measurements have been carried out applying a load of 30 kg, according to standard ASTM E92-72. Indentation fracture toughness K_{IC} has been estimated by applying the Palmqvist model to cracks generated by indentation, using the Shetty equation [32]. For the study of crystalline phases X-ray diffraction (XRD) technique was used (Bruker Theta model D8 advance apparatus, fitted with a Cu filament). Scanning range (2θ) was varied from 20º to 90º and ICDD PDF-2 (2004) database was used for phase identification. The XRD analysis was carried out on the section perpendicular to uniaxial pressed direction.

Results and discussion

Figure 1 shows FESEM images of the general morphology of nanocrystalline WC-12Co commercial powders. In these photographs, it can be seen that although the powders are forming agglomerates with an average size around 500 nm (Figure 1a), the WC average grain size in the WC-12Co mixture is around 30-80 nm (Figure 1b).

Once the powders are put into the mould it is important to have information about the shrinkage of the sample. In the case of SPS sintering, this information can be obtained from the expansion or contraction of the system during the cycle. The evolution of displacement (piston travel) in function of time, pressure and temperature during SPS cycle for the three compositions studied is shown in Figure 2. None of the curves shows an expansion in the compact, so in contrast with Cha et al. [30] has reported, there is no evidence of the formation of liquid phase during the sintering.

The addition of inhibitors does not significantly affect the contraction experimented during the SPS cycles. Only the mixture with VC added exhibited a delay in the displacement curve in comparison with the composition without additives. However, the maximum difference does not exceed 3%. It can be noted that more than 50% of the displacement happens during the pressure step until the maximum pressure is applied (80 MPa). It is in the second part of the heating step, from 650 to 1100 ºC, where it can be distinguished the differences in their behaviour. From this results, a more difficult densification for the sample with VC as assistive can be expected.

The relative density, porosity and WC average grain size of the mixtures fabricated by SPS, HIP and vacuum are shown in Table 2. Materials consolidated by SPS and HIP present a higher relative density compared with that obtained by vacuum, even if the final sintering temperature is considerable lower. This revealed the effectiveness of both pressure assisted sintering techniques, SPS and HIP, in the solid state densification. This good densification results obtained for all the compositions tested in this work confirm that the selected consolidation temperature was correct for allowing the plastic flow of cobalt under pressure. This binder plastic deformation, leading to rearrangement of WC nanograins and diffusion phenomena, are the fundamental mechanisms considered for densification in the absence of liquid phase [10].

Materials without inhibitors (N) consolidated by SPS and HIP are fully densified, while all the samples with additives show a low residual porosity, more pronounced in the materials with VC (NV). This result is agreed with the behaviour observed during SPS sintering. The incomplete densification in the solid state by inhibitors effect is associated with the limitation of the diffusion phenomena and migration of Co [5]. However, density values obtained by the SPS technique are much higher than those

observed in the literature [15, 33, 34]. This is probably due to smaller particle size and increased pressure used during sintering process. If the particle size is smaller, the increase in surface area allows the diffusion phenomena in a higher degree and the final density is closer to the theoretical value.

XRD results show no evidence of η phase (Co_3W_3C or Co_6W_6C) formation in any of the compositions sintered by the three consolidation techniques. The absence of secondary phases confirms the efficacy of the addition of free carbon on the carbon content control of the material sintered in solid phase, even by rapid sintering processes. Figure 3 shows the XRD pattern of the NV composition after consolidation. It can be noted the peak height of WC (0001) plane in the material sintered by SPS is higher than in the samples obtained by other two processes. This indicates a certain degree of orientation of WC grains in the materials sintered by SPS, with a preference orientation of (0001) crystal planes perpendicular to uniaxial pressed direction.

The microstructure of materials consolidated by SPS and HIP can be observed in Figure 4. In both processes, a microstructural inhomogeneity can be appreciated, which is typical for the solid phase sintering, with Co segregations and lack of wettability. This fact improves the interactions between carbides, promoting coalescence phenomena that are responsible for the grain growth [35,36].

In the absence of inhibitors, the SPS technique has allowed obtaining materials with the finest microstructure. This is due to the combination of low sintering temperature, similar to HIP process and a very short processing time. These are the optimal conditions for limiting grain growth if we consider that no additives are being used, because high temperature for liquid formation is avoided and long time that promotes

grain growth are suppressed. Nevertheless, in these conditions, densification would be also hindered. The near full density SPS samples obtained reveal that under the suitable experimental conditions densification without grain growth can be reached. The inhibitors addition, especially VC, has been clearly demonstrated as an effective method for controlling the grain growth during WC sintering. In this work this strategy has been employed for SPS and HIP sintering techniques in order to combine the additives effect with low sintering temperature. The efficiency of both inhibitors is more significant in the HIP process. The combination of VC addition (NV) and consolidation by HIP has allowed obtaining near-nanocrystalline cemented carbides, with an average grain size of 122 nm WC. This microstructure is one of the finest reported in literature [35].

The lesser effect of inhibitors in the SPS process is due to the limitation of diffusion phenomena as a result of the shorter processing times, which makes it difficult the adequate distribution and location of the additives. The mechanisms of growth inhibition are the subject of many research studies [10,15-18]. The effect of VC and Cr_2C_3 on the WC grain growth inhibition has been explained in the presence of the liquid phase by limiting of the solution-reprecipitation mechanisms. This is due to the V and/or Cr dissolution in the cobalt which reducing the solubility of WC in the liquid phase. The inhibitory action of these additives in the solid state is not fully clear. Studies realized suggest the formation of a V or Cr rich thin interfacial layer which suppresses the WC dissolution. This film on the surface of WC grains contributes to the resistance to the diffusion of W [35]. As it has been previously explained, the short processing times for SPS sintering allowed the suppression of grain growth by limiting the diffusion phenomena. When the additives are used, they need a diffusion step or a reaction time in order to operate. As in the SPS sintering this time is too short, the

additives efficiency is lower in comparison with the other sintering techniques. It is important to note that when the results of SPS sintering are observed isolated, it can be seen the effect of the additives. Then, the combination of SPS sintering and inhibitors use improves the grain growth control. In any case, more studies are needed to understand the roles of these carbides on grain growth inhibition during solid state sintering.

Diameter equivalent distribution of the WC grains of NV composition consolidated by SPS and HIP by are plotted in Figure 5. For this composition, the grains percentage with nanometric size was about 30% for the material obtained by SPS while it was more than 55% for sintered by HIP. In both cases 99% of the grains present a size that is less than 400 nm. From these results it can be concluded that there are two kinetic effects for controlling the WC grain growth. On one side the self diffusion phenomena that leads to grain growth and in the other side, the inhibitor particles diffusion that allows the WC grain growth control by different mechanism proposed in the literature. It is important to highlight his result because it opens the possibility of getting the smallest particle size in dense WC by an accurate design of the sintering cycle.

Finally, the hardness and fracture toughness values of the three compositions consolidated by SPS, HIP and vacuum sintering are compared in Figure 6. Materials without inhibitors (N) sintered by SPS and HIP reach hardness values >20% higher than the corresponding sintered in vacuum. This result is directly related with the full densification and smaller grain size obtained by these techniques. The higher hardness values of the sample without inhibitor (N composition) sintered by SPS and HIP, make that the increase obtained with the inhibitors addition (NCr and NV compositions) are less significant than in the samples consolidated by liquid phase conventional sintering.

However, hardness values about 2100 HV_{30} has been achieved for NV composition sintered by HIP, which represents an increase of 15% compared to the mixture without inhibitor, N composition. This improvement in hardness is accompanied by a loss of fracture toughness, due probably to loss of strain capacity of the binder as a result of decreasing mean free path and/or the dissolution of VC. In any case, the fracture toughness values obtained for the hardest materials are close to 10 MPa $m^{1/2}$. It is well understood that the hardness of cemented carbides materials is inversely proportional to its grain size and that the fracture toughness is inversely proportional to the hardness, although the relationship between the hardness and fracture toughness may not be linear when the grain sizes are extremely fine. Therefore, a finer grain size usually results in lower fracture toughness. However, for nanostructured metallic alloys and ceramics, it has been noted that the mechanisms of strengthening are different because of the large volume fractions of grain boundaries. The deformation mechanisms depend on grain boundary sliding and diffusion-controlled processes [37]. Thus, the effect of interfaces on the deformation mechanisms and/or change in the crack propagation path could contribute to better fracture toughness.

Conclusions

WC-12Co-VC/Cr_2C_3 cemented carbides near fully dense were obtained by SPS and HIP in solid phase at 1100 ºC. The addition of inhibitors, especially VC, has been demonstrated to be an efficient method for controlling the grain growth in the solid state, even by rapid sintering processes. However, in SPS technique, a lesser effect of both inhibitors has been observed due to extremely short processing time, thus limiting the appropriate distribution and location of the additives. The good microstructural

control achieved by VC addition and HIP sintering at low temperature has allowed manufacturing near-nanostructured materials with average WC grain size of 120 nm. As result, materials with an attractive combination of properties were obtained: hardness values about 2100 HV_{30} and fracture toughness values close to 10 MPa $m^{1/2}$.

Acknowledgement

The work is supported financially by the Spanish Ministry of Science and Innovation by means of the project MAT 2006-12945-C03-C02 and MAT 2009-14144-C03-C02.

References

[1] Jia C., Sun L., Tang H., Qu X. Int. J. Refract Met Hard Mater 2007;25:53-6.

[2] Kim H.C., Shon I.J., Yoon J.K., Don J.M. Int. J Refract Met Hard Mater 2007;25:26-52.

[3] Kim H.C., Jeong I.J., Shon I.J., Ko I.Y., Donh J.M. Int J Refract Met Hard Mater 2007;25:336-40.

[4] Bartha L., Atato P., Toth A.L., Porat R., Berger S., Rosen A. J Adv Mater 2000;32:23-6.

[5] Carroll D.F., Int J Refract Met Hard Mater 1999;17:123-32.

[6] Fang Z.Z., Eason J.W., Int J Refract Met Hard Mater 199;13:297-303.

[7] McCandlish L.E., Kear B.H., Kim B.K. Nanostruct Mater 1992;1:119-25.

[8] Porat R., Berger S., Rosen A., Nanostruct Mater 1996;7:429-36.

[9] Zhang L., Madey T.E. Nanostruct Mater 1993;2:487-93.

[10] Azcona I., Ordonez A., Sanchez J.M., Castro F., J Mater Sci 2002;37:4189-195.

[11] Agrawal D., Cheng J., Seegopaul P., Gao L., Powder Metall 2000;43:15-16.

[12] Breval E., Cheng J.P., Agrawal D.K., Gigl P., Dennis M., Roy R., Papworth A.J., Mater Sci Eng A 2005:391:285-95.

[13] Huang S.G., Vanmenensel K, Li L. Mater Sci Eng A 2008;475:87-91.

[14] Zhao S.X., Song X.Y., Zhang J.X., Liu X.M., Mater Sci Eng A 2008;473:323-9.

[15] Sivaprahasam D., Chandrasekar S.B., Sundaresan R. Int J Refract Met Hard Mater 2007;25:144-52.

[16] Zhao H.F., Zhu L.H., Huang Q.W. Rar Met Mater Eng 2005;34:82-5.

[17] Sun L., Jia C.C., Lin C.G., Cao R.J., J Iron Steel Res Int 2007;14:85-9.

[18] Huang S.G., Li L., Vanmeensel K., Van der Biest O., Vleuges J., Int. J. Refract. Met. Hard Mater 2007;25:417-22.

[19] Kim H.C., Jeong I.K., Shon I.J., Ko I.Y., Doh J.M. Int J Refract Met Hard Mater 2007;25:336-40.

[20] Kim H.C., Oh D.Y., Shon I.J. Int J Refract Met Hard Mater 2004;22:197-203.

[21] Kim H.C., Shon I.J., Jeong I.K., Ko I.Y., Yoon J.K., Doh J.M. Met Mater Int 2007;13:39-45.

[22] Dubensky E.M., Nilsson R.T., Dense fine grained monotungsten carbidetransition metal cemented carbide body and preparation thereof. US patent 5773735; 1996.

[23] Michalski A., Siemiaszko D. Int J Refract Met Hard Mater 2007;25:153-8.

[24] Wang X., Fang Z., Sohn H.Y., In: Proceedings of the 2007 International Conference on Powder Metallurgy & Particulate Materials, Denver, US; 2007. p. 08-1.

[25] Silva A.G.P., Souza C.P., Gomes U.U., Medeiros F.F.P., Ciaravino C., Roubin M. Mater Sci Eng A 2000;293:242-6.

[26] Morton C.W., Wills D.J., Stjernberg K. Int J Refract Met Hard Mater 2005;23:287-93.

[27] Carroll D.F., Int J Refract Met Hard Mater 1999;17:123-33.

[28] Lin C., Kny E., Yuan G., Djuricic B., J Alloy Comp 2004;383:98-102.

[29]. Huang S.G, Vleugels J., Li L., Van der Biest O., Proceeding of the 16th international Plansee Seminar. Reutte, vol 2; 2005. p 378-89.

[30] Cha S.I., Hong S.H., Kim B.K. Mater Sci Eng A. 2003:351:31-8.

[31] Michalski A., Siemiaszko D. Int J Refract Met Hard Mater 2007;25:153-8.

[32] Shetty D., Wright I., Mincer P. J Mater Sci 1985;20:1873-82.

[33] Zhu L.H., Huang O.W., Zhao H.F. J Mater Sci Let 2003;22:1631-3.

[34] Sun L., Ha C.C., Xian M. Int J Refract Met Hard Mater 2007;25:121-4.

[35] Fang Z.Z., Wang X., Taegong R., Hwang K.S., Sohn H.Y. Int J Refract Met Hard Mater 2009;27:288-99.

[36] Fang Z., Maheshwai P., Wang Z., Sohn H.Y., Griffo A., Riley R. Int J Refract Met Hard Mater 2005;23:249-57.

[37] Gleiter H., Nanostruct Mater 1992;1:1-19.

Figure and Table Captions

Figure 1. FESEM micrographs of the nanocrystalline WC-12Co mixture: a) general image, b) detail of the aggregates.

Figure 2. Variations of displacement in a function of the time, pressure and temperature during SPS cycles for the three compositions (N, NCr, NV).

Figure 3. XRD pattern of composition NV sintered by SPS, HIP and vacuum.

Figure 4. FESEM micrographs of consolidated materials by HIP: a) N, b) NCr, c) NV and SPS: d) N, e) NCr, f) NV.

Figure 5. Diameter equivalent distribution of the WC grains in NV materials sintered by SPS and HIP.

Figure 6. Vickers hardness and fracture toughness values of all the compositions in function of sintered process.

Table 1. Designation and composition of the powder mixtures.

Tabla 2. Density, porosity and sintered grain size of the mixtures consolidated by SPS, HIP and vacuum.

Table 1

Table 1.

Designation	Starting mixture	Additives (wt.%)		
		Cr_2C_3	VC	C
N	WC-12wt.% Co	0	0	0.8
NCr	WC-12wt.% Co	1	0	0.8
NV	WC-12wt.% Co	0	1	0.8

Table 2

Table 2.

Material	Consolidation process	Relative density (%)	Porosity	Sintered grain size (nm)
N	SPS 1100ºC-80MPa-5min	99.94	<A02 <B02	216
NCr	SPS 1100ºC-80MPa-5min	99.79	A04 B02	207
NV	SPS 1100ºC-80MPa-5min	98.95	A06 B02	154
N	HIP 1100ºC-120MPa-30min	99.97	<A02 <B02	253
NCr	HIP 1100ºC-120MPa-30min	99.85	A02 B02	214
NV	HIP 1100ºC-120MPa-30min	99.43	A02 B02	122
N	Vacuum 1400ºC-30min	99.20	A02 B02	747
NCr	Vacuum 1400ºC-30min	99.08	A04 B04	398
NV	Vacuum 1400ºC-30min	98.42	A04 B04	178

Figure 1

Click here to download high resolution image

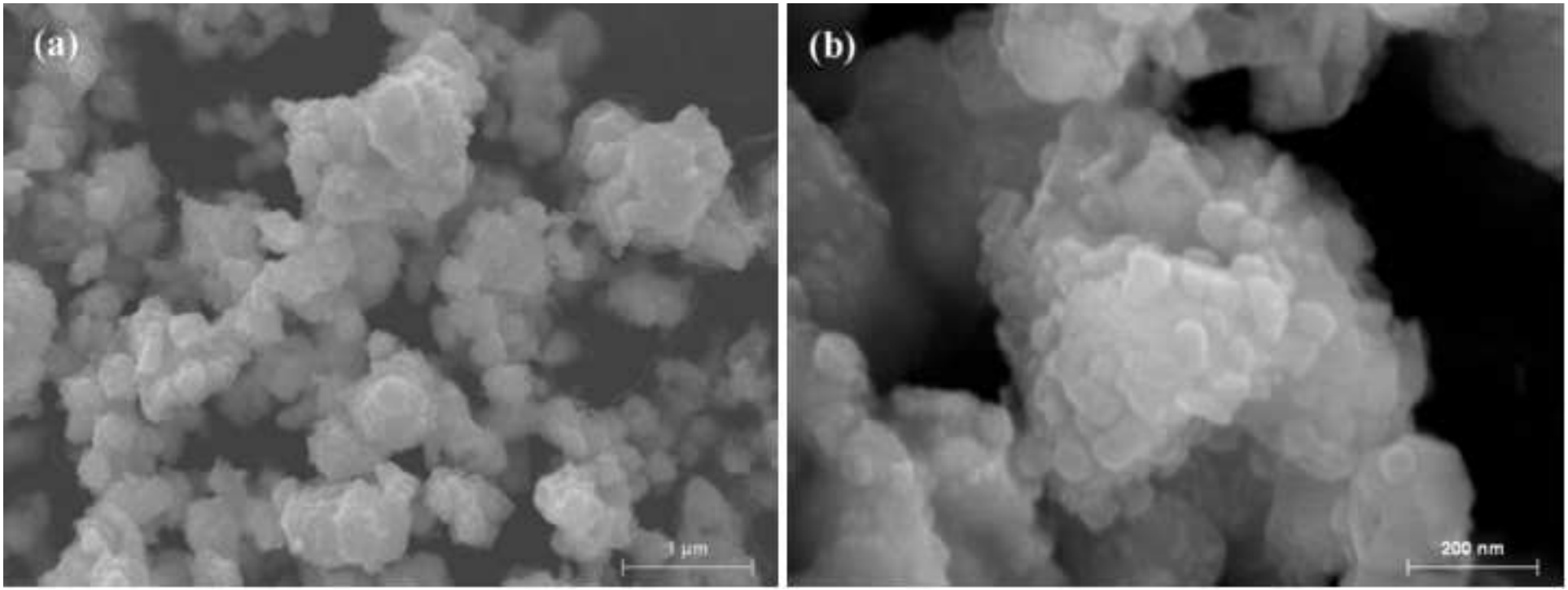

Figure 2

Click here to download high resolution image

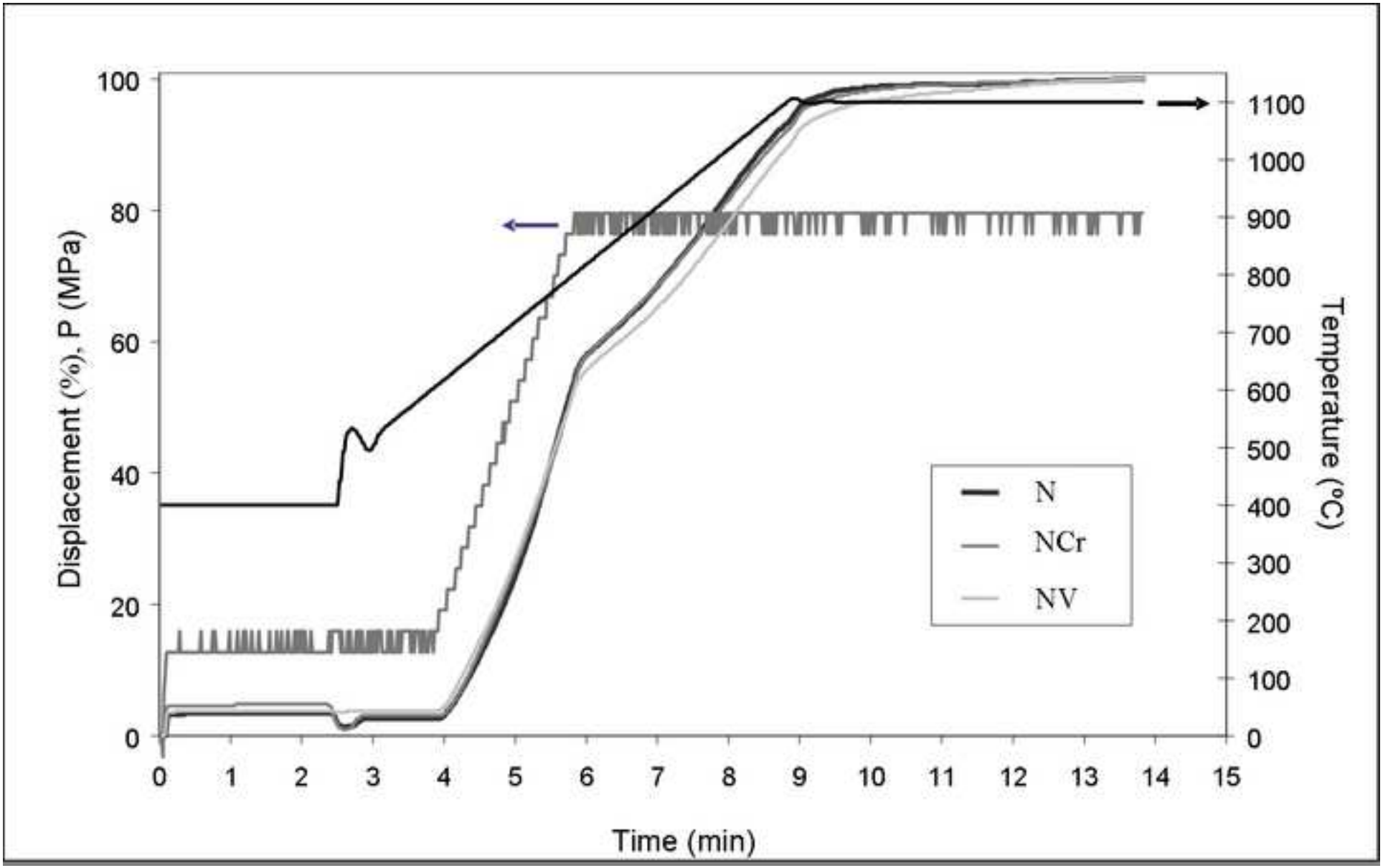

Figure 3

Click here to download high resolution image

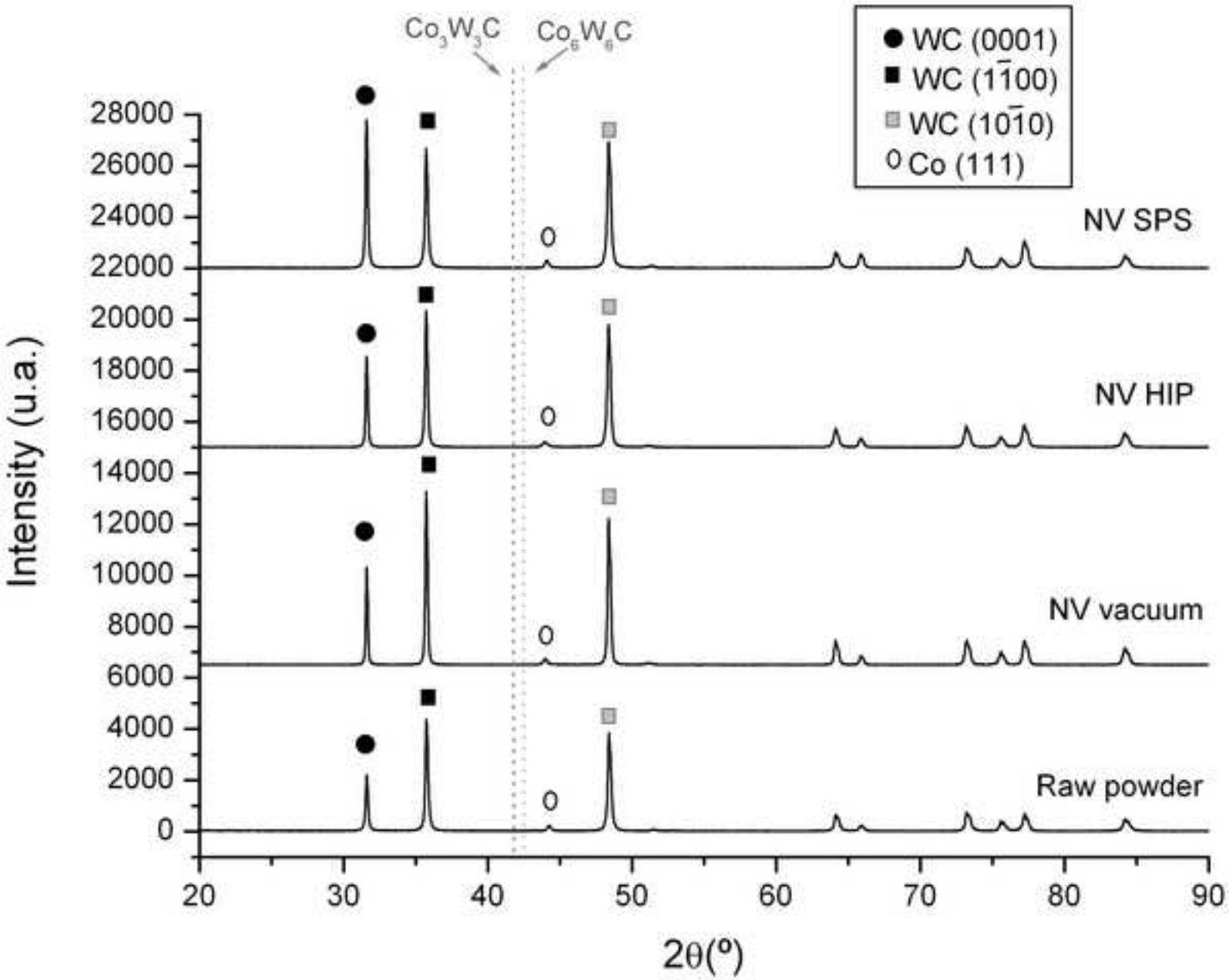

Figure 4

Click here to download high resolution image

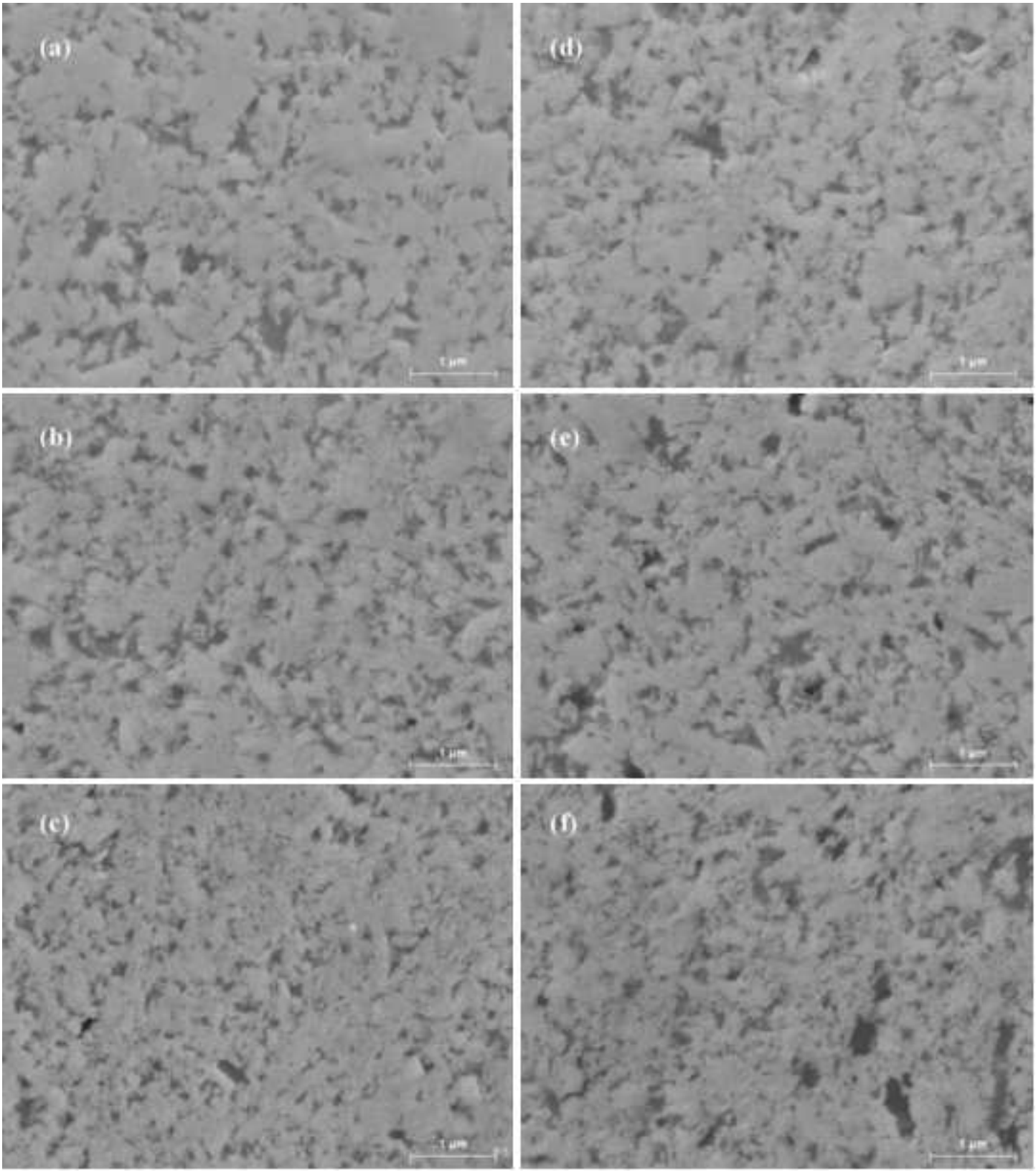

Figure 5

Click here to download high resolution image

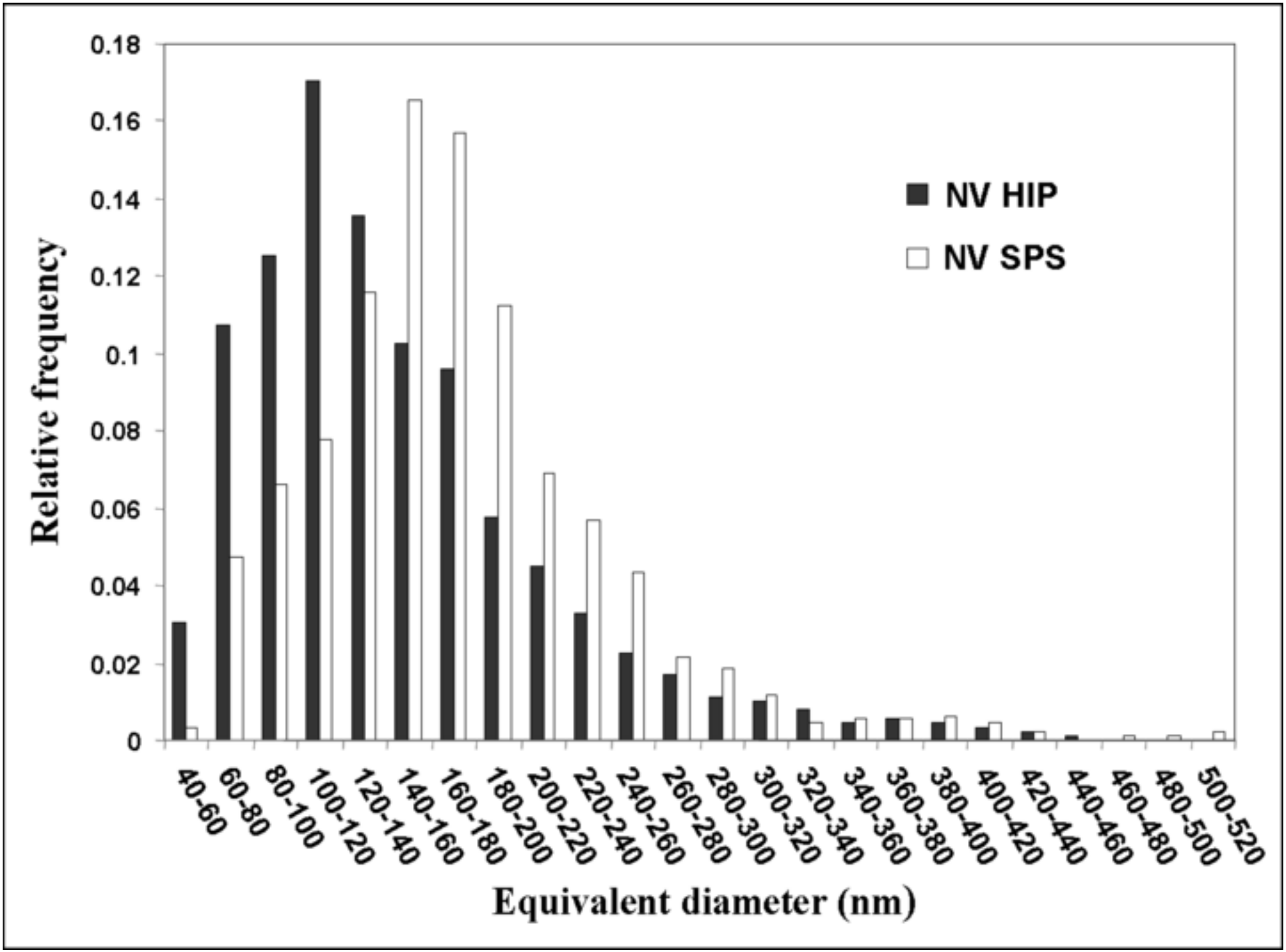

Figure 6

Click here to download high resolution image